Supporting Information

SI Materials and Methods

Plant materials and reporter constructs. The *clv3-2* allele in the La-*er* background has been previously described [24,25]. The *wus-1* and *wus-6* alleles have been described previously [16]. The *AHK4*$_{pro}$*::GFP* line in Columbia (Col-0) background has been previously described [26]. The *WUS*$_{pro}$*::dsRED-N7* lines have been previously described [10]. The *WUS*$_{pro}$*::WUS-2xYFP* construct in the T-DNA vector pMLBART [27] conferring Basta resistance in plants is composed of 3.33 kb of upstream regulatory sequence from the *WUS* gene fused to the WUS coding region and 2 tandem copies of YFP followed by the N7 nuclear localization sequence [28] with 1.31 kb of *WUS* 3'-untranslated sequence. The *WUS*$_{pro}$*::mTFP-ER* and *CLV3*$_{pro}$*::mTFP-ER* reporters are composed of 4.4 kb of upstream regulatory sequence and 1.5 kb 3'-untranslated sequence for *WUS* and 3.3 kb upstream regulatory sequence and 1.5 kb 3'-untranslated sequence for *CLV3* in the binary vector pMOA33 conferring kanamycin resistance. For double transgenic plants with various reporters, *WUS*$_{pro}$*::WUS-2xYFP* was crossed into respective backgrounds as previously described [29]. For the construction the *LOG*$_{pro}$ reporter lines, 4.5Kb of the up- stream promoter region and 1.5Kb of sequence downstream of the ORF stop codon were cloned into the T-DNA vector pMOA conferring hygromycin resistance. Into these constructs a 2x version of Ypet with a N7

(2xYpet-N7) nuclear localization sequence inserted between the various *LOG* gene regulatory regions. Reporter lines were subsequently crossed into mutant backgrounds.

Gene expression analysis. RNA was harvested from shoot apical tissue (~0.5 cm from the shoot apex) using the RNeasy Mini Kit (Qiagen). cDNA was synthesized from 1 mg DNase1 (invitrogen) treated total RNA. Quantitative real-time PCR was done using SYBR green (Quantance, SensiMix). Data was analyzed using the $\Delta\Delta C_t$ method normalized to tubulin expression. Primer sequences available upon request.

Plant growth and hormone treatment conditions. Plants were grown as previously described [29]. Cytokinin treatments with N6-benzylaminopurine (BAP; Sigma–Aldrich Co., St. Louis, MO) were performed as previously described [10]. For analysis of floral organ number, plants were treated 2 times at one-week intervals at the onset of bolting. Flowers of at least 10 plants were counted for *wus* mutant floral organ number. We counted organs within each flower until the SAM terminated. At least two independent biological experiments were performed for each genotype. For the analysis in Figure 5, *clv3-2* mutants and wild type plants in were treated once every third day. Phenotypic analysis was performed on soil. We tested whether exogenous auxin could influence the *AHK4* expression domain by testing the responsiveness of the *AHK4*$_{pro}$*::GFP* reporter in shoots and roots of intact plants to treatment with 10μM or 25μM of both indole-3-butyric acid (IBA, Sigma) or the synthetic auxin 2,4-D (Sigma) in liquid MS media for 12 hours. In addition, we cultured root and shoot explants for 24hrs on MS plates containing 1mM, 100μM, or 10μM IBA. In Figure S6, tissue explants were cultured on MS plates for 6 days with 500μg/L of the synthetic auxin 2,4-D. Imaging was performed

as previously described [29]. Membranes were stained with FM4-64 dye unless otherwise noted [29].

Imaging conditions. Callus and regenerating shoots were imaged directly on respective media. For each marker line, at least 10 samples were imaged to confirm that observed patterns were representative of respective markers. The lipophilic dye FM4-64 (Molecular Probes) was used at a concentration of 10 µg/ml to demarcate cell membranes. All imaging was done using a Zeiss 510 Meta laser scanning confocal microscope with a 10x air objective, 63x water dipping lens, or a 40x water dipping lens using the multi-tracking mode. Specific sets of filters used for the respective markers were similar to those already described [10]. Projections of confocal data were exported using Zeiss LSM software. Scanning electron microscopy was performed as described previously [29].

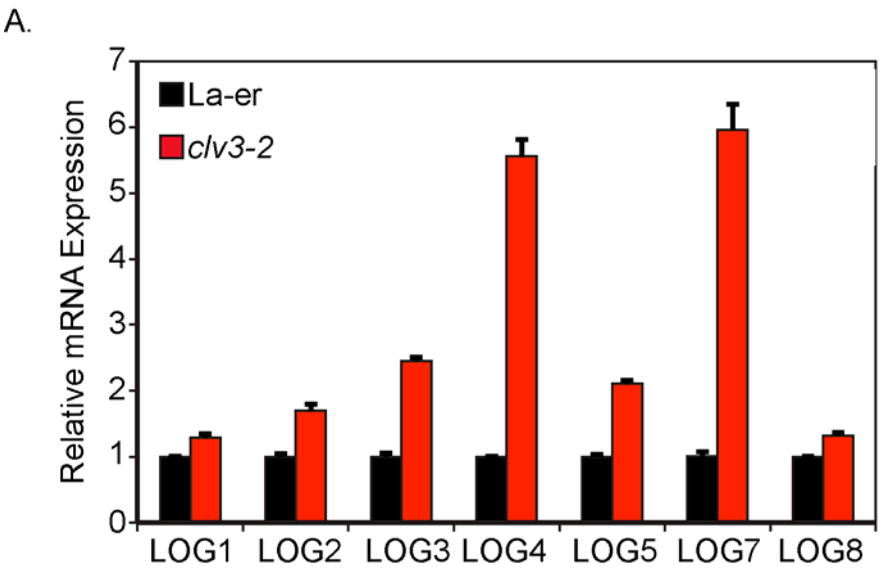

Figure S1. **qRT-PCR of *AtLOG* in shoot apical tissue.** (A) Relative expression levels of the six *AtLOG* genes in the La-er or the *clv3-2* mutant backgrounds.

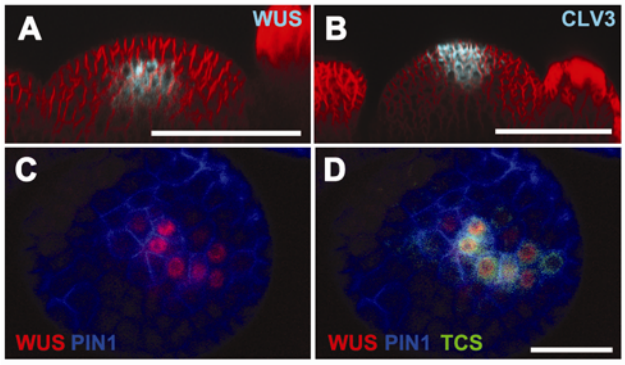

Figure S2. Distribution of cytokinin synthesis, perception, and signaling relative to *WUS* within the SAM. (A) Longitudinal view of WUS_{pro}::mTFP-ER reporter, (B) $CLV3_{pro}$::mTFP-ER reporter. (C) Top view of WUS (WUS_{pro}*::WUS-2xVenus*, red) and (D) TCS_{pro}*::GFP* (green) in the SAM and floral meristem. In C-D $PIN1_{pro}$*::PIN1-GFP* (blue) marks cell membranes. Scale bar represents 50µm in A, B and 20µm in C, D.

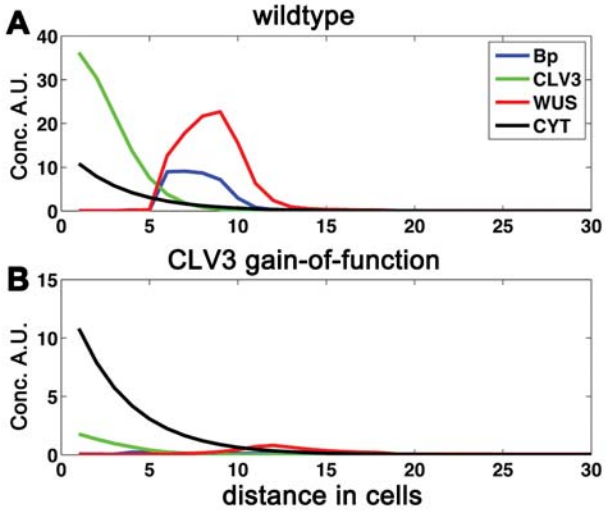

Figure S3. Loss of meristem function for gain of function CLV3.

(A,B) show simulations for the model for the CLV3 gain of function. The plots display WUS, CLV3, Cytokinin signaling (phosphorylated B Type ARR's -- Bp) and Cytokinin along the apical-basal axis in wild type (A) and the CLV3 gain of function (B). In B, the green curve for CLV3 represents the promoter activity (see SIAppendix).

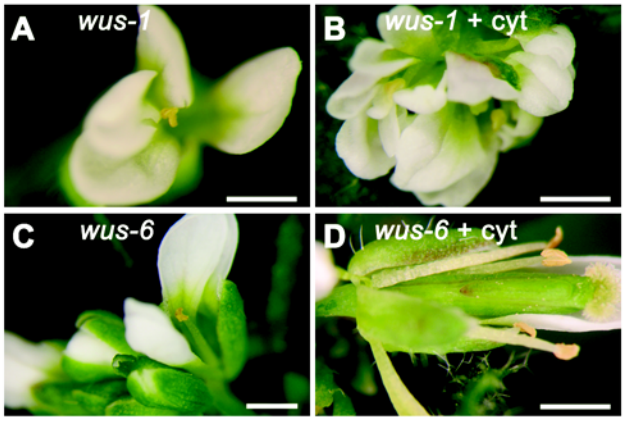

Figure S4. **Exogenous cytokinin rescues floral meristem termination in the hypomorphic *wus-6* promoter insertion mutant.** (A) Mock treated *wus-1* mutant flower missing inner floral organs. (B) Cytokinin treated *wus-1* flowers have supernumerary outer organs but still lack inner organs. (C) Mock treated *wus-6* mutant flower missing inner floral organs. (D) Cytokinin treatment leads to a full complement of floral organs in *wus-6* flowers. Scale bars represent 1mm in A, B, D and 0.5mm in C.

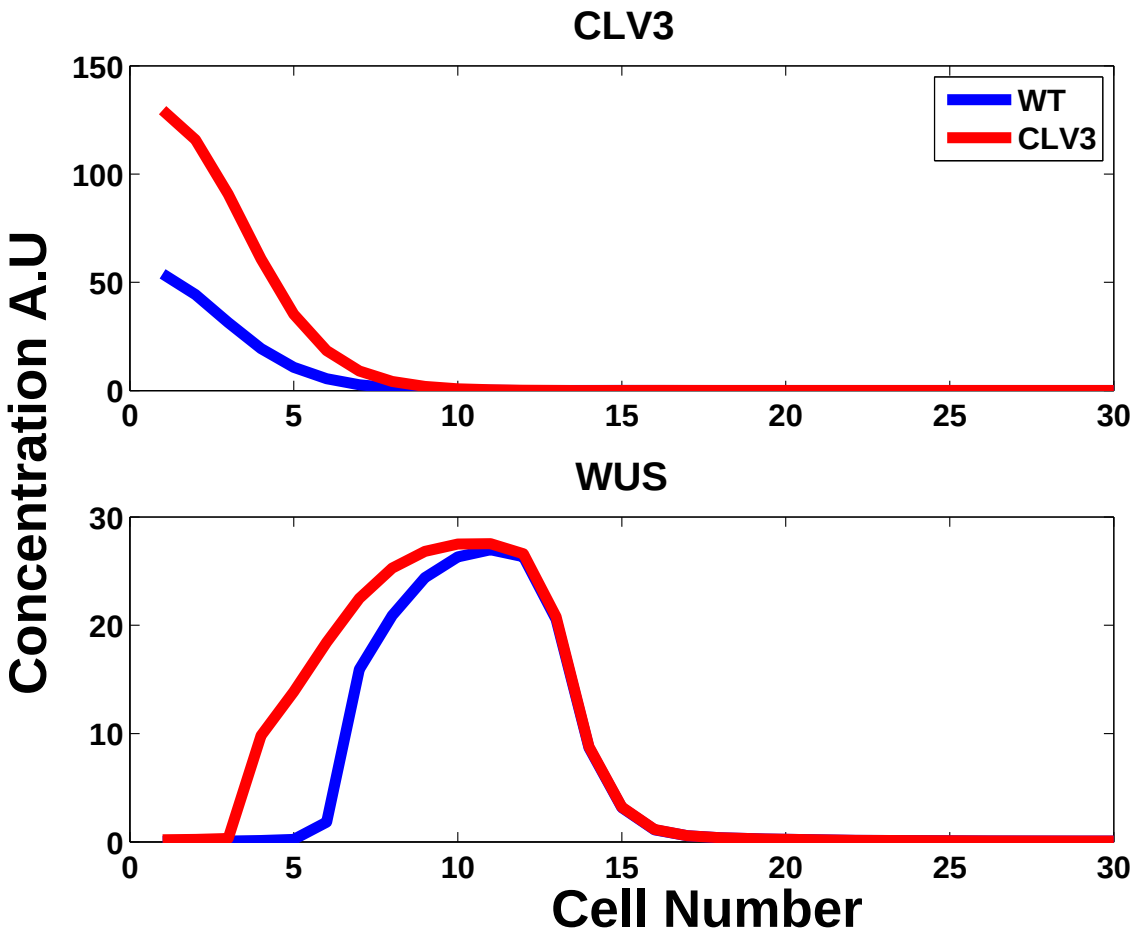

Figure S5. Model simulations for *clv3* loss-of-function. *clv3* loss-of-function simulations (blue=functional CLV3, red=*clv3* loss-of-function). The upper plot shows simulations of CLV3 concentration along a column of cells (apical cell=0, basal most cell=30). The plots represent CLV3 promoter activity (see SIAppendix). The lower plot shows simulations of WUS concentration along the same column of cells.

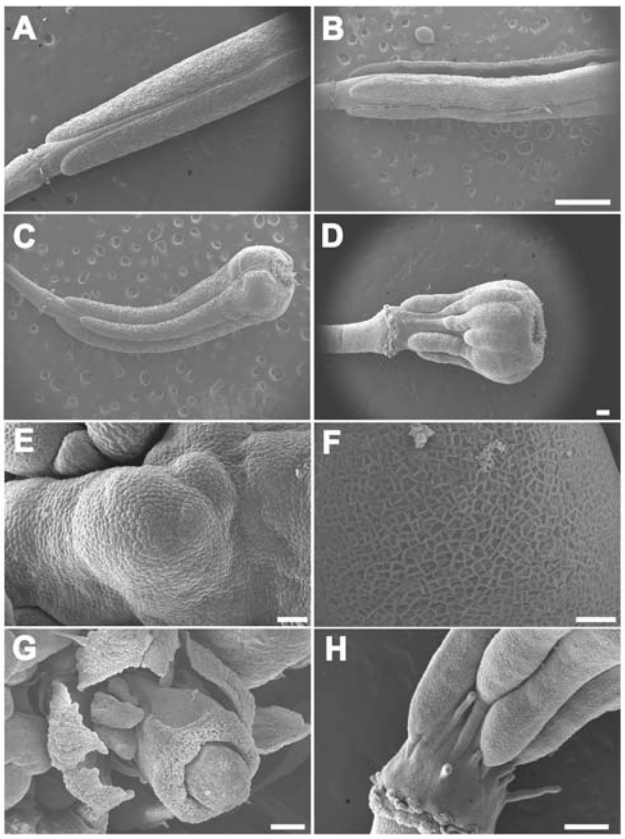

Figure S6. Cytokinin treatment enhances carpel number phenotypes in the *clv3-2* background. Scanning electron images of wild type mock-treated (**A**), wild type cytokinin-treated (**B**), *clv3-2* mutant mock-treated (**C**), and *clv3-2* mutant cytokinin-treated (**D**) carpel number. Cell size in *clv3-2* mock (**E**) and *clv3-2* cytokinin treated (**F**) SAMs. Abnormal grow in the center of cytokinin-treated *clv3-2* mutant gynoecium (**G**) and at its base near the pedicel (**H**).

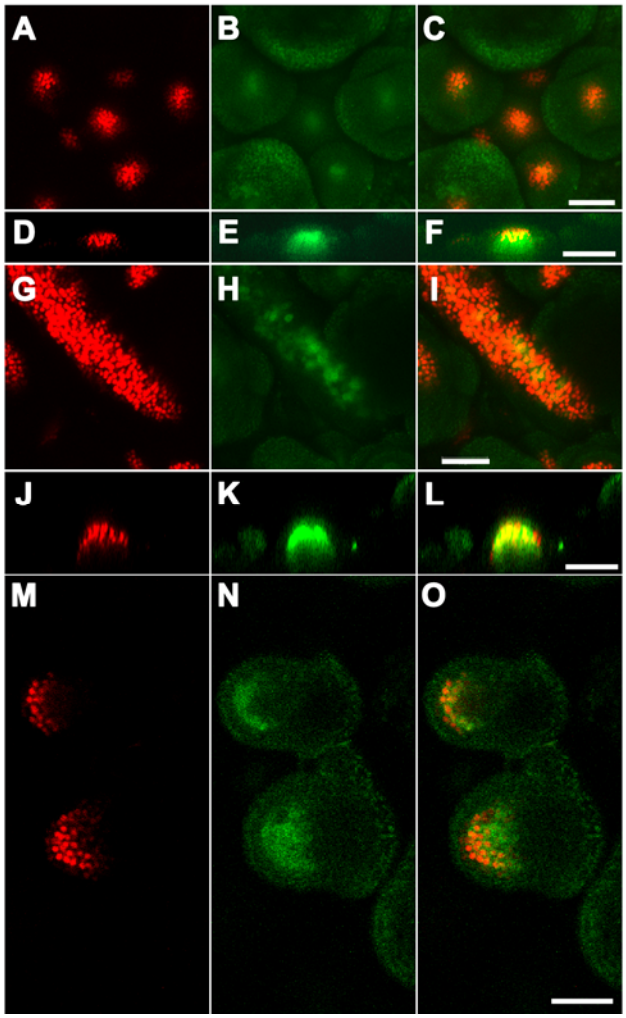

Figure S7. Cytokinin receptor and *WUS* expression in the *clv3-2* mutant. (A-C) top down and (D-F) transverse views of *WUS_{pro}::DsRed-N7* (red) (A), *$AHK4_{pro}$::GFP* (green) in wild type. (G-I) Lateral expansion of *WUS_{pro}::DsRed-N7* (red) (A), *$AHK4_{pro}$::GFP* (green) in the *clv3-2* mutant. (J-L) Longitudinal section of *WUS_{pro}::DsRed-N7* (red), *$AHK4_{pro}$::GFP* (green) and *$AHK4_{pro}$::GFP; WUS_{pro}::DsRed-N7* in a *clv3-2* mutant SAM. (M-O) Longitudinal section of *WUS_{pro}::DsRed-N7* (red), *$AHK4_{pro}$::GFP* (green) and *$AHK4_{pro}$::GFP*; *WUS_{pro}::DsRed-N7* in *clv3-2* mutant floral meristems. Scale bars represent 50µm.

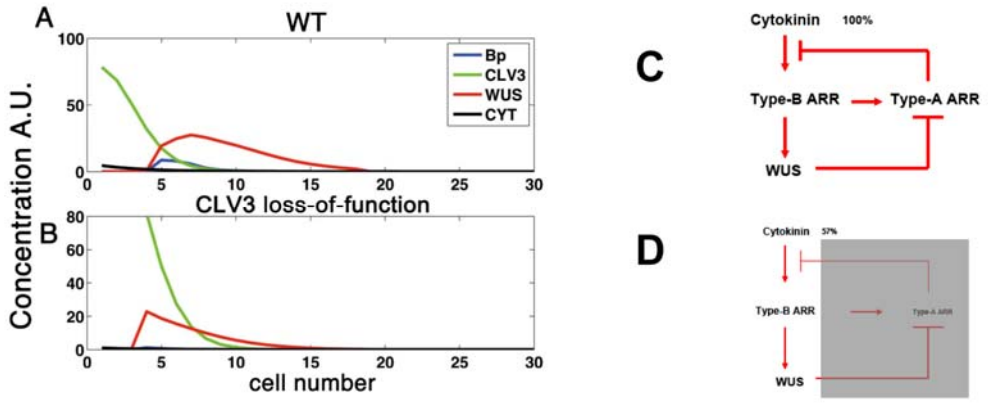

Figure S8. **Modeling results for WUS expression compared to cytokinin signaling in wild type and for loss of function CLV3 for the negative cytokinin biosynthesis model .** (A,B) show simulations for the model in which we assume WUS negative feedback on cytokinin synthesis, assuming a greater affinity of Type-B ARR to the WUS promoter (greater efficiency of WUS induction by cytokinin). The plots display WUS, CLV3, Cytokinin signaling (phosphorylated B Type ARR's -- Bp) and Cytokinin along the apical-basal axis in wild type (A) and the clv3 loss of function mutant (B) (here CLV3 represents promoter activity). (C) and (D) show cartoons of the regulatory network involving Type-A ARR, Type-B ARR and WUS, suggesting that in (D), low levels of cytokinin could potentially still maintain WUS, since WUS is strongly induced by cytokinin thereby keeping Type-A ARR low, which in turn allows WUS to be induced. WT (wild type).

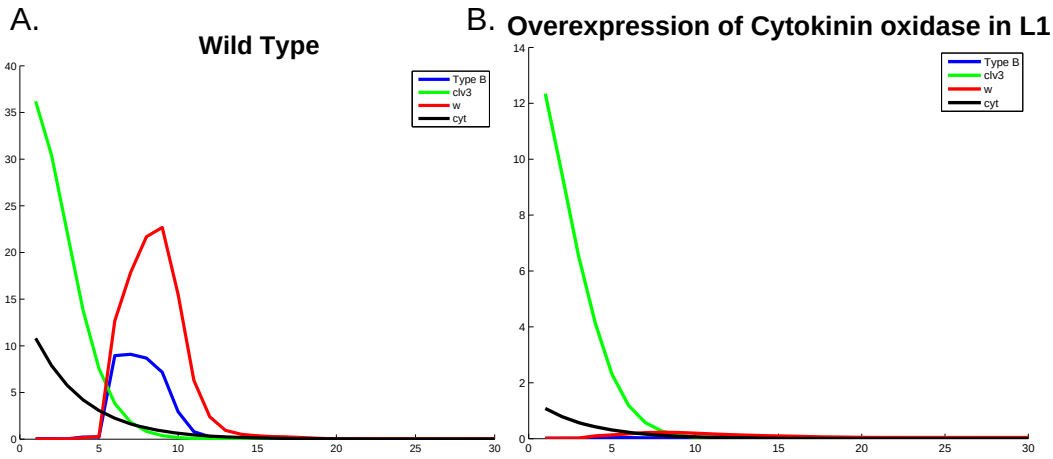

Figure S9. **Modeling results for a case where a cytokinin degradative enzyme is expressed in the L1 layer of the SAM maintenance.** (A,B) show simulations for a model where we have expressed a cytokinin degradative enzyme, such as a member of the *CYOTKININ DEHYDROGENASE/OXIDASE* family, in the L1 layer of the SAM. The plots show WUS, CLV3, cytokinin, and cytokinin signaling (phosphorylated type-B ARR) in a wild type and L1 specific overexpression of a CKX enzyme. In (A) the proper apical-basal patterning occurs. When CKX is expressed in the same cell producing the apical cytokinin signal, the plot for cytokinin signaling, WUS, and CLV3 are no longer maintained. The simulation in (B) mimics a SAM termination phenotype as observed for loss of *log* function in rice or multiple loss of *log* function in Arabidopsis.

Video Captions:

Video S1 Movie of growth and division, displaying the maintenance of CLV3, WUS, Type A ARR & Type B ARR spatial profiles, assuming all cells express cytokinin receptors.

Video S2 Movie of growth and division, displaying the maintenance of CLV3, WUS, Type A ARR & Type B ARR spatial profiles, as well tracking number of cell divisions and the receptor region, assuming a cytokinin receptor profile which is propagated by the stochastic receptor model.

Computational Supplement

Introduction

In the supplement, we outline details of the computational model. In particular we will discuss in order,

- Cytokinin Perception Spatial Circuit Dynamics
- Typical Timescales for Perturbations.
- Cell Growth and Division Rules.
- Combining Simulation of Gene Expression and Cell Growth.
- CLV3, cytokinin dependent growth rate.
- Cytokinin Receptor Domain Propagation Model.
- Guide to interpreting movie 2
- Cytokinin biosynthesis feedback models.
- Robustness Studies.
- CLV3 loss/gain of function.

Cytokinin Perception Spatial Circuit Dynamics

In an earlier publication [1] we have described a simplified model of the signaling and transcriptional network through which cytokinin signaling induces WUS expression. We also refer the reader to the references in [2], for a review of cytokinin signaling.

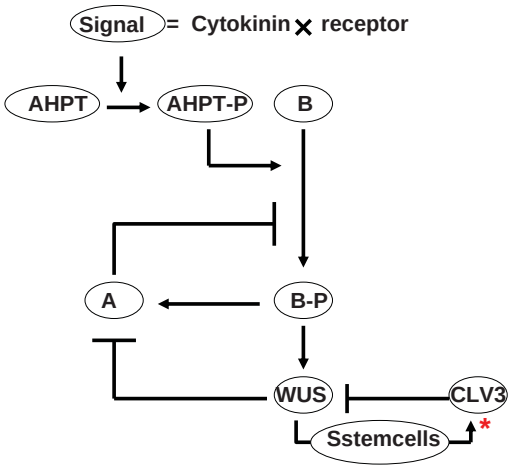

Figure 1: A schematic of the cytokinin perception signaling-genetic network. AHPT–Arabidopsis histidine phosphotransfer protein, B–Type B Arabidopsis Response Regulator(ARR), A–Type A Arabidopsis Response Regulator(ARR), WUS, CLV3, Sstemcells. The red star indicates that the Sstemcells signal also regulates a signal which makes cells competent to express CLV3(see Equation 1)

Referring to the schematic Figure M1, we assume that the signal which phosphorylates the histidine transfer proteins (AHPTs), is a product of the cytokinin and the cytokinin receptor concentrations within a cell. The signal is transduced by $AHPT_P$ and further phosphorylates the Type B ARRs. B_P is transcriptionally active and activates transcription of Type A ARRs, as well as WUS. The Type A ARRs negatively regulate signaling, giving rise to a negative feedback loop. WUS suppresses transcription of the Type A ARRs, which gives a positive feedback loop (these two consecutive negative feedbacks give a positive feedback). WUS activates a diffusible signal, Sstemcells, which activates CLV3, the latter represses WUS. In our earlier model [1] we had also explicitly included CLV1, but here we have simplified the network by retaining only the essential WUS-CLV3 feedback loop for simplicity. In addition to the above, we extend our previous model by explicitly introducing 3 new diffusible species which are experimentally motivated:(1) Observations suggest (see

Figure S2A,B from the main text) that the first 3-4 cells at the apical region express CLV3, we implement this in our model in the following way: the cell at the very tip of the shoot apex expresses a signal, CLV3signal, which diffuses down into the lower layer of cells, and which we assume makes cells competent to express CLV3. Since the gradient of this signal falls of exponentially [1], only the top few cells can express CLV3. (2) A stem cell maintenance signal Sstemcells, which emanates from the WUS region, and which activates CLV3 as well as the CLV3signal. (3) Cytokinin is assumed to be produced by the first cell, and simply diffuses into the lower layers. In the model, cytokinin biosynthesis does not depend on WUS activity. However, in a later section, we have explored the consequences of making the biosynthesis of cytokinin regulated by the WUS, through the Sstemcell signal. In this section, where the template is assumed to be fixed, cells express cytokinin receptors, with a distribution such that cells 5-18 express high levels of cytokinin receptors(this follows from our observations of the AHK4 receptor [1]) [2]. Later when we consider growth and cell division, we discuss a dynamic model to propagate the receptor domain. We now cast these assumptions into a mathematical form such that they describe the protein levels within each of the cells of the cellular template, which we have chosen to be the apical-basal slice of the shoot meristem(see Figure 1 from the main text). Within each cell we solve for the following circuit, where the index i is the cell index, which runs from $1:N$(at the moment N is fixed, i.e we consider a static template, later we add growth and cell division to this template)

$$\begin{aligned}
\frac{d[AHPT_P]_i}{dt} &= (\frac{[signal]_i[AHPT]_i}{K_{h1}+[AHPT]_i}) - \frac{v_{h1}[AHPT_P]_i}{K_{h2}+[AHPT_P]_i}, \\
\frac{d[B_P]_i}{dt} &= (\frac{[AHPT_P]_i[B]_i}{K_1+[B]_i})(\frac{1}{1+\alpha[A]_i}) - \frac{v_1[B_P]_i}{K_2+[B_P]_i}, \\
\frac{d[A]_i}{dt} &= \frac{a_0+a_1[B_P]_i}{1+a_1[B_P]_i+a_2{[WUS]_i}^n} - \gamma_a[A]_i, \\
\frac{d[WUS]_i}{dt} &= \frac{b_0+b_1[B_P]_i}{1+b_1[B_P]_i+b_2[CLV3]_i} - \gamma_w[WUS]_i
\end{aligned}$$

[1] The profile has a typical length scale of $\sqrt{D/\gamma}$, where D is the diffusion constant and γ is the degradation rate

[2] We have also considered a simpler situation where all cells express the same levels of cytokinin receptors.

$$
\begin{aligned}
\frac{d[CLV3signal]_i}{dt} &= \alpha_1 \frac{\hat{a(1)} d_s [Sstemcells]_i}{1 + d_s [Sstemcells]_i} - \gamma_{clvs} [CLV3signal]_i \\
&\quad + D_{CLV3signal} ([CLV3signal]_{i+1} + [CLV3signal]_{i-1} - 2[CLV3signal]_i) \\
\frac{d[CLV3]_i}{dt} &= \alpha_2 \left[\frac{d_1 [CLV3signal]_i}{1 + d_1 [CLV3signal]_i} \right] \left[\frac{d_2 [Sstemcells]_i}{1 + d_2 [Sstemcells]_i} \right] - \gamma_{clv} [CLV3]_i \\
&\quad + D_{CLV3} ([CLV3]_{i+1} + [CLV3]_{i-1} - 2[CLV3]_i) \\
\frac{d[Sstemcells]_i}{dt} &= \alpha_3 \frac{d_w [WUS]_i}{1 + d_w [WUS]_i} - \gamma_{sc} [Sstemcells]_i \\
&\quad + D_{Sstemcells} ([Sstemcells]_{i+1} + [Sstemcells]_{i-1} - 2[Sstemcells]_i) \\
\frac{d[Cyt]_i}{dt} &= \hat{a(1)} C_r - \gamma_{cyt} [Cyt]_i + D_{Cyt} ([Cyt]_{i+1} + [Cyt]_{i-1} - 2[Cyt]_i)
\end{aligned}
\tag{1}
$$

where the $[signal] = [Cyt][receptor]$, which we assume to be expressed at some level in all cells; $\hat{a(1)} = 1$ only for the first cell($i = 1$), and $\hat{a(1)} = 0$ for all $i \neq 1$. The total amount of AHPT and Type B ARR in their two different forms obey, $AHPT + AHPT_P = 10, B + B_P = 10$. We refer the reader to [1], which discusses the first four equations for $[AHPT_P], [B_P], [A], [WUS]$ [3], however for making this supplement self-contained, we briefly describe each term.

- **AHPT** Histidine phosphotransfer proteins $AHPT$ are phosphorylated by the signal ($[Cyt][receptors]$), to the state $AHPT_P$ with the total number of proteins conserved $AHPT + AHPT_P = 10$.

[3]Throughout we assume transcription factor dynamics is modeled based upon a thermodynamic model for transcription [5, 6, 7, 8], which typically gives gene regulatory functions as sigmoidal shaped curves (see above equations) We also model transcription and translation as one combined process. The following simple example will illustrate how sigmoid functions arise in transcriptional dynamics. Let x be the concentration of a transcription factor which transcribes for a gene G, which exists in two states g_0–open, g_1–bound by x. These represent the relative occupancy of the gene, $g_0 + g_1 = 1$. We assume x binds and unbinds at a high rate, much faster than the transcription process itself. Then assuming thermodynamic equilibrium for the reaction, $x + g_0 \rightleftharpoons g_1$, with k_{-1}, k_1 as the backward and forward rates, with the equilibrium constant $K = \frac{k_1}{k_{-1}}$, we obtain $g_1 = K g_0 x$, which from the conservation equation $g_0 + g_1 = 1$, gives the fraction of the occupied gene g_1. The transcription rate is assumed to be proportional to this fraction, since it represents genes being occupied and ready to transcribe. Hence the transcriptional rate T is,

$$
T \propto \frac{Kx}{1 + Kx}. \tag{2}
$$

- B_P Type B ARRs (response regulators) are phosphorylated by $AHPT_P$, to B_P with the total number of proteins conserved $B + B_P = 10$. In the equations for $AHPT_P$, B_P, we have assumed enzymatic dephosphorylation as well as phosphorylation, and hence we use Michaelis Menten forms for the equations.

- **Type A ARR** The Type A ARRs are assumed to be transcribed by a target of cytokinin signaling which we will assume to be Type B ARR, and also suppressed by WUS, with multiple WUS binding sites on As promoters [3].

- **WUS** transcription is promoted by a cytokinin-regulated transcription factor which here we model as a B Type ARR B_P. B_P could be replaced by any transcription factor activated by cytokinin that promotes transcription of WUS and Type A ARRs.

- **[CLV3signal]** We assume that this is a diffusible signal that is produced only by the first cell ($a\hat{(}1)$)and is further regulated transcriptionally by Sstemcells, the diffusible signal produced by WUS. CLV3signal diffuses into the lower layers, and makes cells competent to express CLV3. Since it is only produced in the top cell, its gradient falls off exponentially, and hence only the first few cells which sense reasonable levels of [CLV3signal] end up expressing CLV3. This is is further implemented as described next,

- **[CLV3]** In the equation for $\frac{d[CLV3]}{dt}$, the first term is a product of two terms: the first term ,$\frac{d_1[CLV3signal]_i}{1+d_1[CLV3signal]_i}$ makes cells competent to express CLV3, the second term $\frac{d_2[Sstemcells]_i}{1+d_2[Sstemcells]_i}$ describes activation of the CLV3 promoter by the stem cell signal, $Sstemcells$. Hence [CLV3signal], which is strong only within the top 3-4, cells guarantees that [CLV3] falls off for cells further away from the apical tip. This implementation is analogous to assuming an AND type of gate for the cis-regulatory logic for stem cells producing CLV3. Another option would have been to assume a heteromeric term like $[CLV3signal][Sstemcells]$ acting as an activator, however, with the lack of any evidence, we used the simplest possible assumption.

- **[Sstemcells]** We assume that WUS activates a diffusible signal [Sstemcells] that maintains stem cells. The latter is assumed to activate CLV3 as well as [CLV3signal](as discussed above).

- **[Cyt]** We assume that the first cell produces cytokinin at a fixed rate(later we allow for positive/negative regulation by [Sstemcells], which would be assuming that WUS somehow regulates cytokinin biosynthesis).

- For the diffusible species, $[CLV3signal]$, $[Sstemcells]$, $CLV3$ and Cyt, the coefficients $D_{CLV3signal}, D_{Sstemcells}, D_{CLV3}, D_{Cyt}$ are passive transport rates.

The above equations are solved with appropriate boundary conditions. We assume zero flux boundary conditions for all species except for cytokinin in the first cell where in simulations which correspond to treatment by cytokinin, we assume a fixed external concentration of cytokinin. We use a fourth order Runge-Kutta numerical solver with a small fixed step size to integrate the above equations until a steady state ($\frac{dx}{dt} = 0$) is reached. We then obtain the profiles of the various species as a function of cell number. The parameter values are displayed in Table M1.

The above equations are solved for an initial template consisting of 30 cells, until they reach steady state. The resulting expression levels of all the species are shown in Figure M2A, B, for the two cases respectively, (i) all cells express equal amounts of receptors, (ii) cells express receptors according to a specified pattern (shown in the receptor profile, Figure M2C). The latter is motivated by images of the AHK4 receptor domain which shows strong expression overlapping the WUS domain [1]. From the figures, we notice that CLV3 (Please note that in our model, since we do not explicitly compute the mRNA levels, this means that the protein level is a read out of the promoter activity. In particular model simulations of a CLV3 loss-of-function/gain-of-function mutant, is implemented by having the CLV3 protein bind with less/more strength respectively to the WUS promoter (lower/higher b_2)). CLV3signal and cytokinin are high in the first 4-5 cells and then fall off. The combination

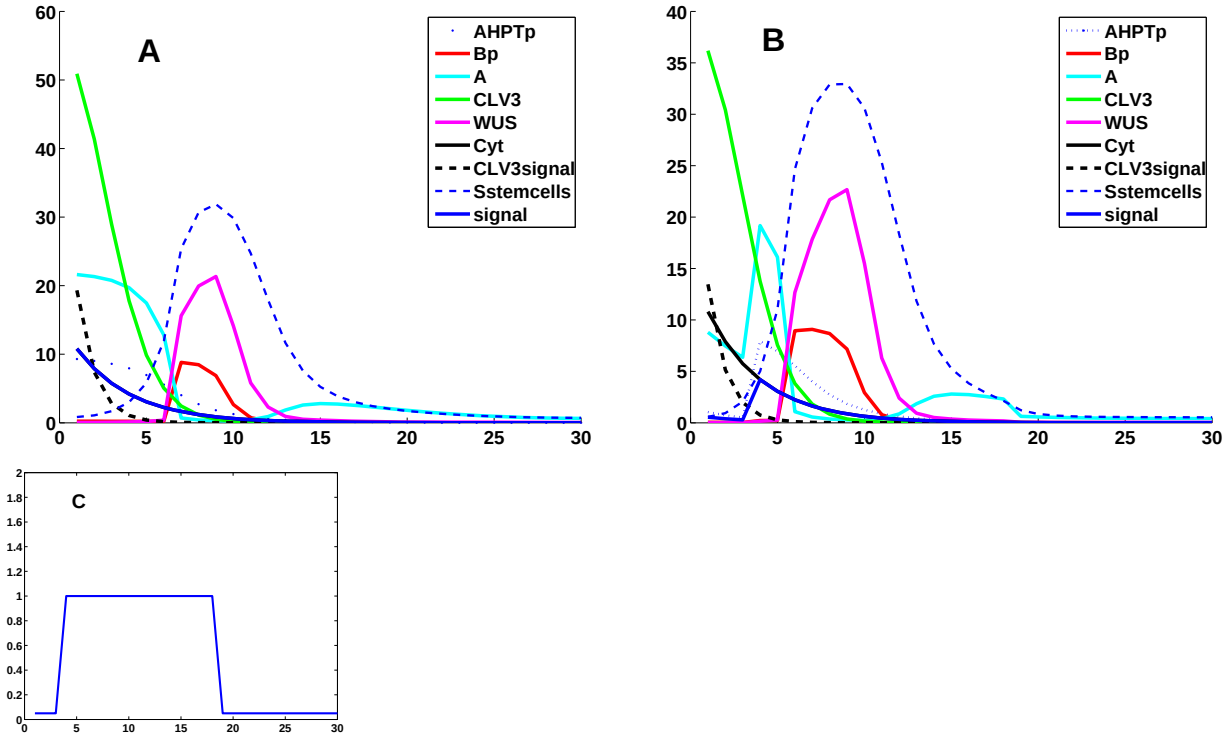

Figure 2: Panel A shows the spatial profile of network components as a function of cell number, apical zone(extreme left), for the case with a constant receptor distribution(corresponding to $receptor = 1$ for all cells. Please note that the curves for signal and Cyt overlap.). Panel B shows the profile for the network components, which was generated by assuming the specific form of the receptor distribution shown in Panel C.

of these profiles determines the WUS profile, which then itself feeds back to further shape the CLV3 profile through the Sstemcells signal. This self-organized network maintains the WUS profile as seen. Further the Type A ARRs surround the WUS domain, and cytokinin signaling (phosphorylated Type B ARRs, Bp) overlap with WUS (as reported earlier [1]). A further point to note is that the WUS pattern does not vary very much for the above two cases considered. The reason is the following. Allowing the stem cells to express receptors does not allow WUS to come on in these cells(which one would expect since cytokinin concentration is high here), since CLV3 is high and would repress WUS. Allowing basally located cells to express receptors would not influence WUS pattern all that much, since cytokinin is at such low levels that WUS induction would be very low. Hence the "wild type" pattern is fairly robust to the receptor distribution.

Typical Time Scales for Perturbations

Here we look at typical time scales for perturbations to the spatial profiles of the network components, i.e how long does it take for the spatial pattern to be established after a perturbation. We can first analyze typical time scales of signaling and gene expression for a much simpler network. Consider the cytokinin perception network, but which is "disconnected" to the CLV3 feedback loop (by removing repression of WUS by CLV3), thereby leading to a loss of communication between cells. We first study the effect of perturbing the level of cytokinin on the levels of $[AHPTP], [BP], [A], [WUS]$. In Figure M3A, cytokinin is rapidly increased to a steady state level within a time scale of $\simeq 30mins$, which results in the rapid phosphorylation of $[AHPT]$ within approximately the same time scale. $[B]$ then gets phosphorylated which leads to transcription of both $[A], [WUS]$. However, since $[A]$ negatively feeds back on signaling, i.e prosphorylation of $[B]$, the temporal profile of $[BP]$ is affected by the rate of gene expression of $[A]$. Moreover, since $[WUS]$ negatively regulates $[A]$, we first get a rapid increase in $[A]$ (since $[BP]$ is transcribing it), followed by a decrease. The time scale for this process is $\simeq 4Hrs$. Hence signaling and gene expression combined take $2-4Hrs$. One would expect that with diffusion, where cells can communicate their position and adjust expression of the network components, these times scales could vary much more. Indeed, in Figure M3 Panel B, we display time scales to establish the same final pattern of network components, considering a perturbation in each cell one at a time. Specifically, each simulation consists of perturbing a given cell by 25% random variation in network components with respect to its steady state value (keeping the values the same in other cells as their steady state values), and then measuring the time for the same final steady state pattern to reestablish. This is repeated several times for each cell, and then for cells between $3-25$. The cells at the apical zone show considerably higher time scales to settle to the same final pattern as compared to the cells in the basal zone because the pattern of many of the network components are higher there and hence much more adjustment has to be made. We have also studied the time scale dependence on the variation of parameters.

Some of the critical parameters which appear to regulate the time scales are the cytokinin production rate C_r, the strength of repression of WUS by CLV3 b_2, and most importantly the passive transport coefficient $D_i, i = 1:4$, for the various diffusible signals. C_r, b_2 determine how fast WUS expression can be established within a cell, whereas D_i determine how fast local changes can be communicated across the cells. To see how D_i determines the speed of establishing a stable pattern after a significant perturbation, we performed the following simulation. We assume that $C_r = 0.1$ is at a very low level, which would correspond to decreasing the cytokinin production rate in the first apical cell, thereby leading to a loss of WUS expression thereby simulating meristem termination (Supplementary Information - Figure S9). Starting from these initial conditions we set $Cr = 1$, and simulate the recovery of the final pattern. In Movie M1 we plot the values of $[WUS]$–red, $[CLV3]$–blue, $[Cyt]$ – black, to show the dynamics of how the recovery takes place. As cytokinin production is restarted, WUS begins to get expressed in the apical cells. This leads to increase in CLV3, which pushes back WUS and the pattern starts to get refined. The time scale is $\simeq 19hrs$, which is longer compared to earlier perturbations. Consider now a new model in which we increase the passive transport rates of all diffusible signals by a factor of 5. Here in this new model, we first set $C_r = 0.1$(simulating loss of meristem), followed by $C_r = 2.5$(simulating the wild type for this new model), then a similar recovery can be seen in Movie M2, with a lower time scale of $\simeq 12Hrs$. Hence the time scales for large perturbations is parameter dependent, and still lower than the typical $24 - 36Hrs$ times scales for division.

Growth and Cell Division

We now explicitly include growth in each of the cells of the above template (we always start our initial template with 30 cells) Each cell's vertical wall is assumed to grow exponentially, $\frac{dL}{dt} = \lambda L$. Here given that cells divide over a period of $24 - 36hrs$, and within this time, the cell length doubles, $\lambda \simeq \frac{ln2}{36} - \frac{ln2}{24} hr^{-1}$. In our simulations we have used the value of $\lambda = 1$, which would correspond to rescaling the simulation time. In a later section we

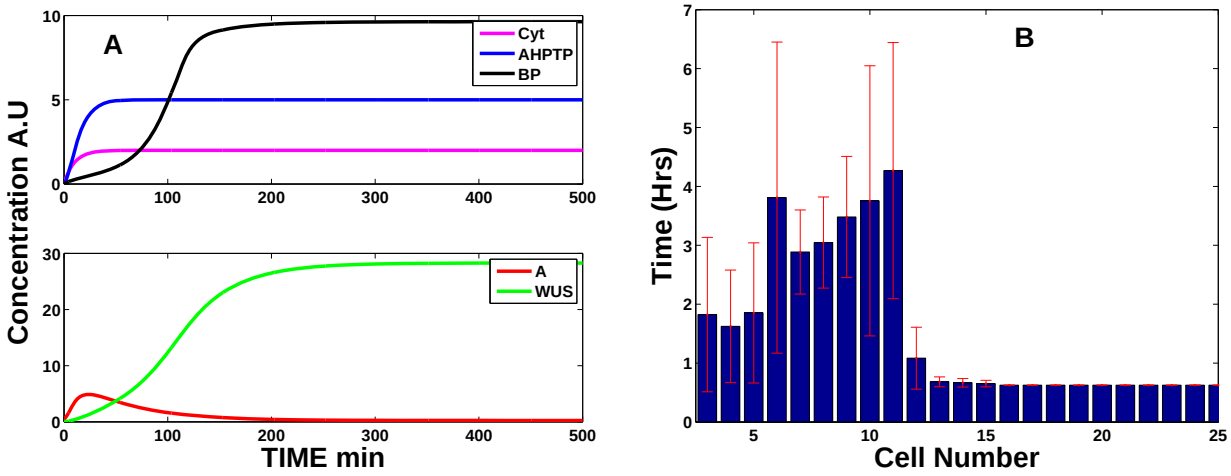

Figure 3: Panel A shows the temporal profile of the single cell cytokinin perception network components as a function of time, for the case when WUS is not suppressed by CLV3. Panel B shows typical timescales for perturbations of the network components by $\pm 25\%$, for each cell, as well as the variation in times scales for a given cell.

make the rate of cell growth dependent on CLV3 and cytokinin. The initial template of cells has been chosen with an average length, $L = 5$ (for ease of visualizing the movies). Each cell has associated with it a length L_d at which it is next going to divide, which is approximately when it reaches twice its initial size, L_i(its size when it was formed on division), hence $L_d \simeq 2L_i$. To obtain L_d, we add to L_i, a length sampled from a Gaussian distribution with $\sigma = .2$, centered at $L_i = 5$. Hence, cells divide asynchronously, since they each reach their threshold for divisions at different times. Upon division, daughter cells partition their lengths into approximately half the original length, with a s.d. of 10%. The cell contents are divided as follows. A given species concentration c_0, is divided into approximately half with a s.d. of $\sigma_c = 25\%$. In particular assuming that for the daughter cells with length l_1, l_2 the species concentration is c_1, c_2, if $c_2 = \sigma_c c_0$, then $c_1 = (\frac{1}{t_1} - \frac{\sigma_c t_2}{t_1})c_0$, where $t_1 = l_1/(l_1 + l_2), t_2 = l_2/(l_1 + l_2)$. This is obtained if we assume that upon division, the total number of molecules is conserved. This is then implemented for all species. For the receptors, we assume that they are partitioned equally between the two cells upon division. For the details of the receptor domain propagation model, see below. In addition we assume

that the first two cells at the tip in our template do not divide, since in reality they represent the cells from the L1 and L2 layer of cells, which are known to divide only anticlinally.

Combining Simulation of Gene Expression and Cell Growth

Here we describe how the cell growth schedule is combined with solving the steady state profiles of the network components. Based upon our analysis of typical time scales for establishing a pattern after a perturbation, we make the assumption that the pattern is established much faster than the time it takes for cell growth to occur. This as we have shown is not always true, since large perturbations could take significantly longer and could begin to approach the cell division time scales. However, we make this assumption to simplify the simulations. Since gene expression occurs faster with respect to growth, it is almost always in steady state. From a simulation point of view, therefore, we can separate the processes of growth and gene expression. We are assuming that as the cell grows, proteins are produced quickly during the entire time period when the cell is enlarging. Hence in our implementation of the growing SAM, we assume that concentration can be held fixed during the simulation of growth. The simulation of the growing SAM follows the following steps, 1. Starting from an initial non-growing cellular template we solve the differential equations (Eq. 1) for the various species until they reach steady state levels. 2. The cells are then made to grow according to the growth rate as described in the text. During growth all cell constituent concentrations are held fixed. 3. If a cell is about to divide, then we stop all growth, and divide that particular cell. We then partition the initial concentration of that cell into its two daughters by the rule given in the text. The new steady state concentrations for all cells are then found by simulating the differential equations for all species. 4. Growth then resumes, once again keeping concentrations fixed until the next division.

Supplementary Movie 1 shows such a simulation of growing and dividing cells, with the two rows marking the network components WUS, CLV3, Type A ARR and Type B ARR,

marked in different colors. Notice that the gross pattern of these components is maintained during growth. This specific simulation assumed that all cells express the same amount of receptors. Supplementary movie 2 is obtained by a simulation which assumes a specific initial profile of receptors and then applies a model of receptor propagation to pattern the receptor domain (see in later section). Here also one observes that the pattern of WUS, etc. are maintained under conditions of growth and cell division. Furthermore, one can compare the initial and final detailed profiles of the network components, to see with what fidelity the pattern is the same. The initial and final patterns for case (i) are virtually the same. More interesting is comparison of these for case (ii), where the receptor domain is determined by the stochastic model, and hence its length can vary. In Figure M4A, we display the final profiles of network components after several hundred cell divisions have occurred. Zooming into the profiles for the first 30 cells(Panel B) shows very similar expression profile to Figure M2B. The maintenance of the patterns occurs even with changes in receptor length (and hence signaling) due to the feedback structure between CLV3, WUS and cytokinin alluded to earlier. The main difference is slight variation in Type A ARR spatial profile, towards the basal direction, which is due to a variation in the cytokinin receptor domain length. This however does not affect the WUS profile very much.

Cytokinin, CLV3 dependent growth model

In our model, CLV3 as well as cytokinin establish a spatial gradient from the tip of the shoot which progressively decreases as one goes deeper into the shoot. We assume that cytokinin enhances growth rate, whereas CLV3 suppresses it. At the very tip, CLV3 is high enough to prevent cytokinin from promoting fast growth. However, for the deeper layers, the CLV3 gradient falls off, and cytokinin can promote rapid growth. Since the cytokinin gradient itself falls off, a break-even point is reached somewhere in the middle where maximum proliferation takes place, as seen in Figure M5. Since the cells are not of very different sizes, we assume that cytokinin and CLV3 affect the growth rate. Hence, we assume that λ, the growth rate

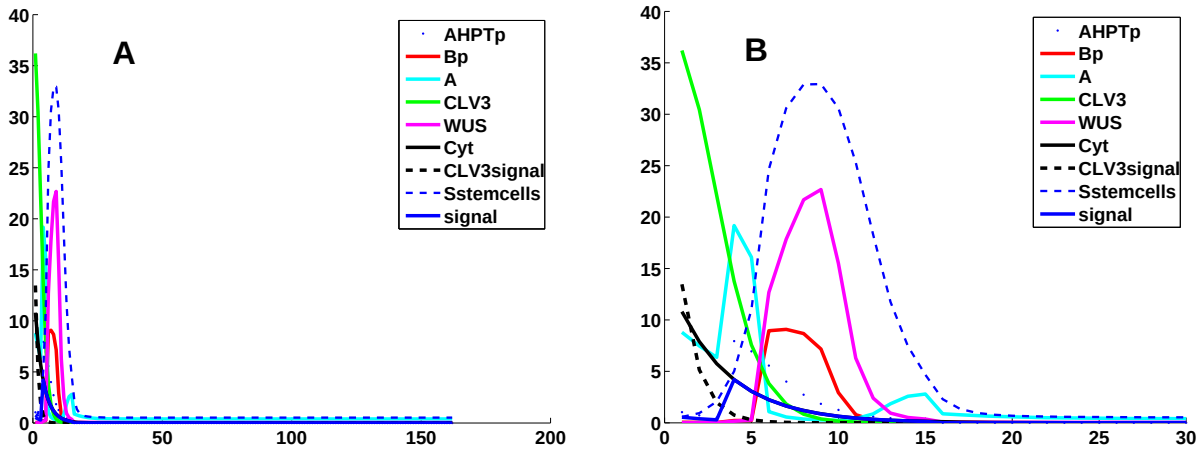

Figure 4: Final profiles of network components after several hundred cell divisions, for the variable receptor domain case.:Panel A shows the "squashed" up profile, which when zoomed into the first 30 cells, Panel B, shows very similar expression profile to Fig M 2B.

is dependent on the following function of CLV3 and cytokinin concentration,

$$f = \frac{1}{(1 + {b_2}^4[CLV3]^{n_1})} \frac{a_2[cyt]^{n_2}}{(1 + a_2[cyt]^{n_2})} \tag{3}$$

with the parameters, $a_2 = 0.1, n_1 = 1, n_2 = 1$, and $b_2 = 1$ (wildtype), $b_2 = 0.1$ (CLV3-loss-of-function). The form of this function is motivated by the following assumptions:(1) CLV3 and

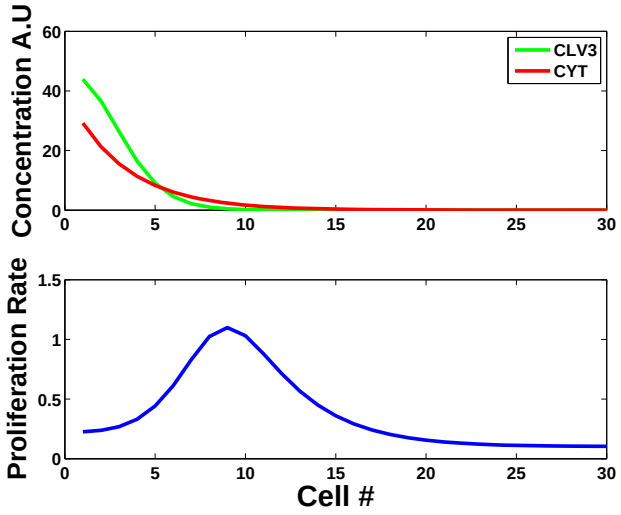

Figure 5: The spatial profiles of CLV3 and cytokinin(upper plot), which determine the growth rate of cells(lower plot), which follows from Eq. 3

cytokinin decrease/increase the growth rate λ respectively, but saturate for high values. Since b_2 determines how strongly CLV3 suppresses WUS, ${b_2}^4$, would give a substantial change in growth rate for the wild type compared to the CLV3 loss of function mutant. (2) Their effect is synergistic, as seen when once compares the sizes of the SEM's for different conditions (Figure 3 A-D main text). For the growth rate we use, $\lambda = 0.1 + 15f$, which corresponds to a maximal value of unity, for cell number 10, from the values of $[CLV3], [Cyt]$, which are displayed in Figure M5, for the wild type model.

Cytokinin Receptor Domain Propagation Model

Observations [1] suggest that the cytokinin receptor domain of expression is maximal several cell layers below the stem cell domain(the first 3-4 cells). Thereafter, cells further below lose expression of the receptors. Hence a simplified picture is that the cytokinin receptor region is several cells long, and somehow manages to retain this pattern as the shoot grows. In our experiments, we have not been able to establish how the cytokinin receptors are regulated, but we have observed that the pattern of cytokinin receptors (through imaging an AHK4 receptor), is propagated perhaps through the action of auxin. Hence in our model we choose a simple model for the cytokinin receptor domain propagation. We assume that each cell in the shoot ultimately arises from the stem cell domain. It is born with a differentiation counter ($d_{count} = 0$). Upon every division, daughter cells inherit the counter and subsequently increases it by one unit to ($d_{count} = d_{count} + 1$). All cells which are **not** stem cells, and are relatively young(have $d_{count} < 6$), are competent to express receptors. Older cells ($d_{count} > 5$) lose receptor expression and are assumed to form part of the differentiated stem. Since younger cells appear just below the stem cell domain, this simple model allows for a receptor expression profile which extends roughly from cell 4-15. However, intrinsic to this model is that, since cell divisions occur randomly, the receptor domain fluctuates in length as a function of time. This can be seen in the figure below (Figure M6) which tracks the receptor domain length over several shoot growth simulations. Considerable variability arises due to

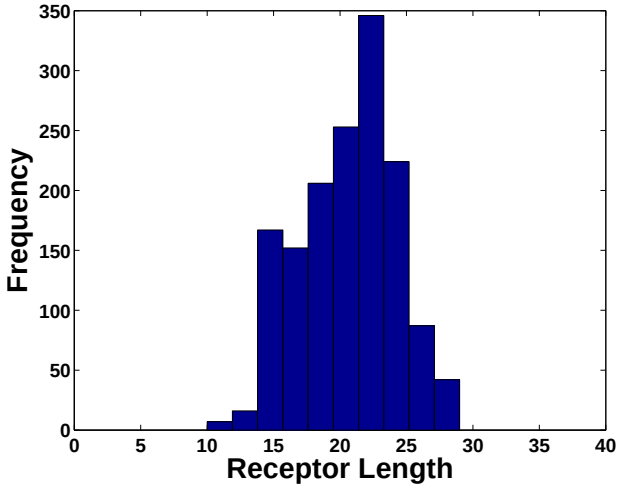

Figure 6: The histogram of the length of the receptor region after several shoot growth simulations show variability.

random and asynchronous division of cells, which continually pushes out new cells from the apical zone in a stochastic way.

Guide to interpreting supplementary movie 2

Movie S2, of growing cells show four different groups of components by coloring the same growing shoot in four different ways. Referring to Figure M7, which shows a screen shot of the movie of shoot growth:

- The first column on the left marks CLV3 and WUS in green and magenta respectively. All other cells are marked as blue.
- The next column, Type-A ARR and phosphorylated Type-B ARR, marked in cyan and red respectively.
- The third column marks out cell divisions, with, (stem cells)red, (1 division)cyan, (2 divisions)green, (3 divisions)magenta, (4 divisions)yellow.
- The last column marks out the receptor region in red.

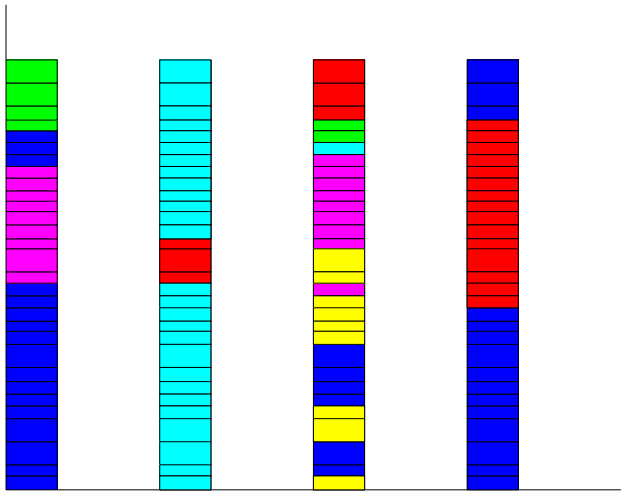

Figure 7: The coarse spatial pattern of key components of the initial template of cells.

Cytokinin biosynthesis feedback models

There are two possible modes of feedback regulation by which WUS can control cytokinin biosynthesis, either by activation, or by suppression. Both these hypotheses are modeled in a simple way as follows. The last equation in Eq. 1, for $\frac{d[Cyt]}{dt}$ is replaced by one of these two equations, depending on which case is being considered. The first case represents WUS feedback to positively regulate cytokinin biosynthesis.

$$\frac{d[Cyt]_i}{dt} = a\hat{(}1)C_r(1 + \frac{a_c[Sstemcells]^2}{1 + a_c[Sstemcells]^2}) - \gamma_{cyt}[Cyt]_i + D_{Cyt}([Cyt]_{i+1} + [Cyt]_{i-1} - 2[Cyt]_i) \tag{4}$$

The second case represents WUS negative feedback of cytokinin biosynthesis,

$$\frac{d[Cyt]_i}{dt} = a\hat{(}1)\frac{C_r}{1 + r_c[Sstemcells]} - \gamma_{cyt}[Cyt]_i + D_{Cyt}([Cyt]_{i+1} + [Cyt]_{i-1} - 2[Cyt]_i) \tag{5}$$

Both of these models are used with the same parameters in Table M1, to generate the curves in Figure 4 A-D (Main Text).

Robustness Studies

The mathematical model of stem cell maintenance extends a previously studied simplified model of cytokinin perception [1] which includes WUS, CLV1, CLV3, AHPT-P, Type B ARRs and Type A ARRs. In the current model we include additional levels of regulations, through 3 new signals, Sstemcells, CLV3signal and cytokinin. In particular, several of the species undergo diffusion. We first discuss parameterizing the passive transport coefficients. Consideration of a diffusing morphogen, with diffusion constant D from a source, which also degrades with rate γ, gives a typical length scale $\sqrt{\frac{D}{\gamma}}$ over which the steady state profile drops exponentially. Since we have selected the degradation rate $\gamma = 0.025$, to be the same for all species, we need to choose appropriate values of the passive transport constants, so as to obtain the appropriate length scales, which according to observations(for example CLV3 extends to approximately 3-5 cells, WUS extends from 5-10 cells). We further make two simplifications in choosing $D's$ for the diffusing species, namely CLV3, Sstemcells, cytokinin, CLV3signal:(1) we assume all proteins share the same passive transport rate,(2) $D_{cyt} > 10 D_{CLV3,..}$(metabolites diffuse faster than proteins [4]). We have selected D, by hand, for all species such that the cytokinin profile extends approximately from cells 1-15, and WUS appears strongly for cells $5 - 15$. Figure M8 describes a robustness study of the CLV3-WUS pattern to variation of D over a 5 fold range (i.e 5 times larger as well as 5 times smaller than the fiducial passive transport coefficient $D = 0.025, D_{cyt} = 0.25$). As can be seen from the plots, for lower D, the WUS peak is closer to the apical domain, which for larger diffusion constants moves basally. This is expected, since, increasing the diffusion constants make both cytokinin and CLV3 reach deeper into the meristem, while at the same time allowing establishment of the pattern. The pattern is very robust to these changes.

In previous work [1], we have explored the robustness of the basic network for cytokinin perception, and hence in this paper we explore the robustness of the other parameters, namely:

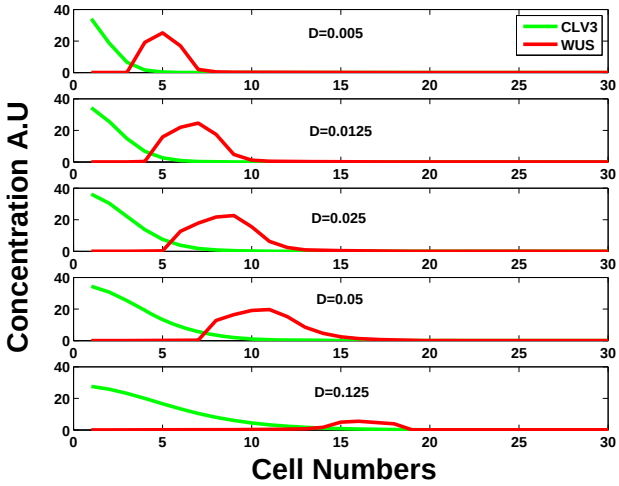

Figure 8: Spatial pattern of WUS and CLV3 for varying passive transport coefficient.

1. α_2 – Production rate of CLV3

2. d_1 – Activation of CLV3 by $CLV3signal$.

3. d_2 – Activation of CLV3 by $Sstemcells$.

4. α_3 – Rate of production of $Sstemcells$.

5. d_w – activation of $Sstemcells$. by WUS

6. C_r – production rate of cytokinin

7. α_1 – production rate of $CLV3signal$.

8. d_s – activation of $CLV3signal$ by $Sstemcells$.

To study the robustness, we use the normalized spatial sensitivity.

Normalized Spatial Sensitivity

For a signaling-genetic network, described by $\frac{dc_i}{dt} = f_i(c_j, p_1, p_2, ...)$, with species concentration c_i, and parameters p_k, one way to study how small changes to parameters affect the

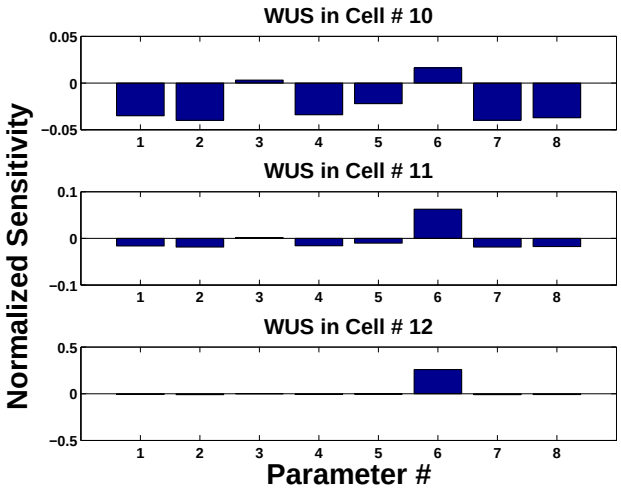

Figure 9: WUS sensitivity in cell numbers 10, 11 & 12

model results is to study the normalized local sensitivity, which is defined as,

$$S_j{}^i = \frac{p_j \partial c_i}{c_i \partial p_j} \tag{6}$$

The rate of change of the steady state value of a species concentration as a function of a parameter is normalized with respect to the steady state value of the concentration and the parameter value. Hence if we increase a parameter by a small amount $\delta\%$, the value of the species concentration increases by $S_j{}^i \delta\%$. Since our template extends over several cells, the sensitivity can be defined both with respect to each individual cell, and hence is a spatially dependent quantity. Hence we define the spatial sensitivity by adding an extra index k, as $S(k)_j{}^i$. Here k refers to cell number, j is the parameter, and i is the species. Since there are 8 species, and 8 parameters, within a cell, the sensitivity S is a 8×8 matrix. Using this definition we can perform the following studies: sensitivity dependence of a given species within a given cell upon all the parameters; and spatial sensitivity of a parameter for any species. In Figure M9 we see WUS sensitivity in three cells $(10, 11\&12)$, which are within the main WUS domain. There are a couple of interesting features to notice,(1) WUS in cell 10 is more sensitive to changes than Cell 11, since the former is close to the apical WUS boundary and hence would be particularly sensitive to changes in expression level

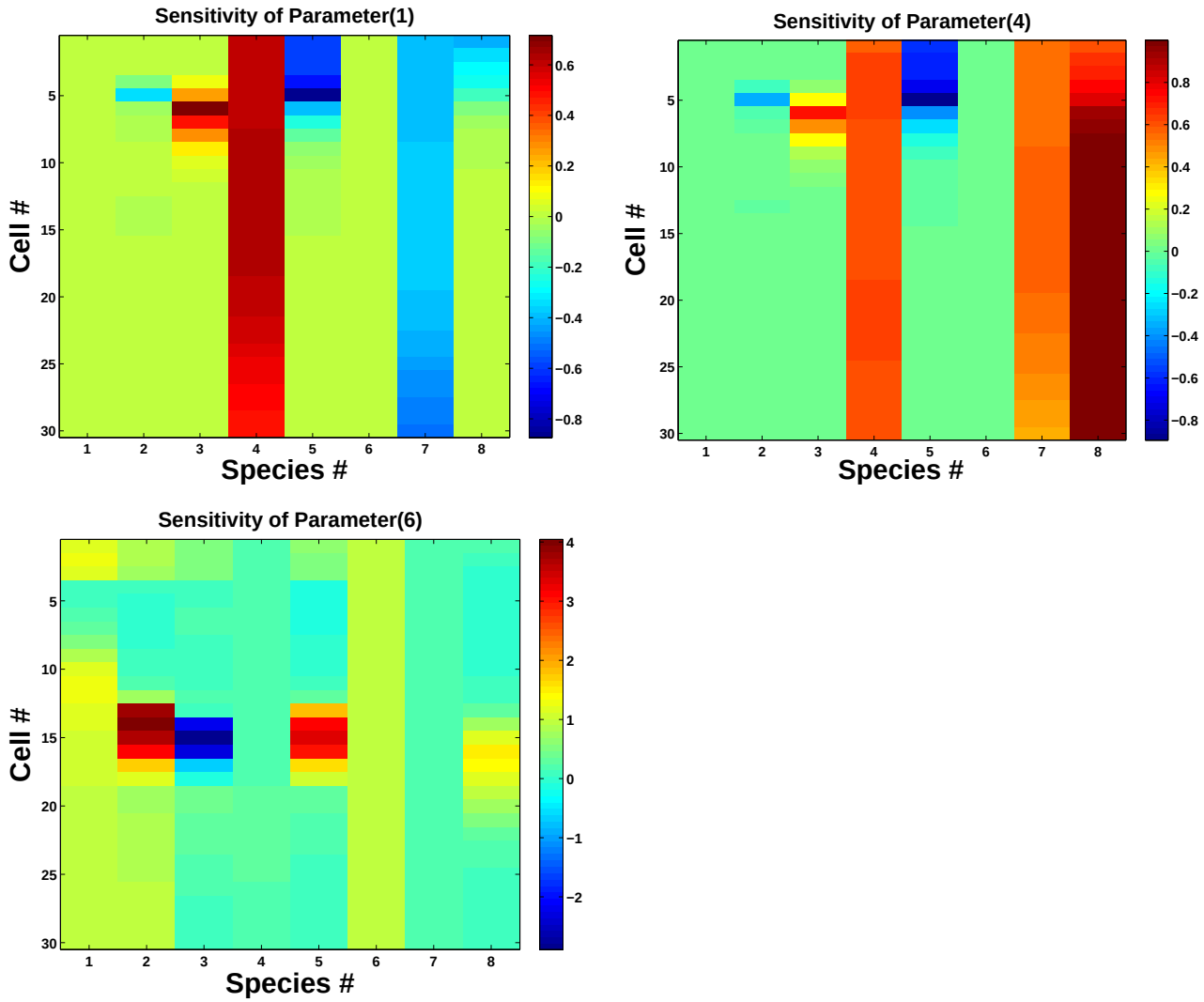

Figure 10: Heat maps of spatial sensitivity for several parameters. The species are numbered $1-8$, and correspond to AHPT-P, B-P, A, CLV3, WUS, cytokinin, Sstemcells, CLV3signal.

with respect to parameter changes, whereas cell 11 is within the WUS domain. (2) The second point is that increasing the majority of parameters lead to negative sensitivity, since increasing any of them(except $3, 6$), lead to increase in CLV3. (3) We see from the figure that for cells 11 and 12, the most sensitive parameter is the rate of cytokinin production. In Figure M10 we show the heat maps, which plot the spatial sensitivity for each species, for three of the relevant parameters (1,4 & 6), which correspond to CLV3, Sstemcells, and cytokinin production rates respectively. In each case we see that the sensitivity in all cells for a particular species is affected. In particular:(1)for CLV3 production rate–CLV3 has

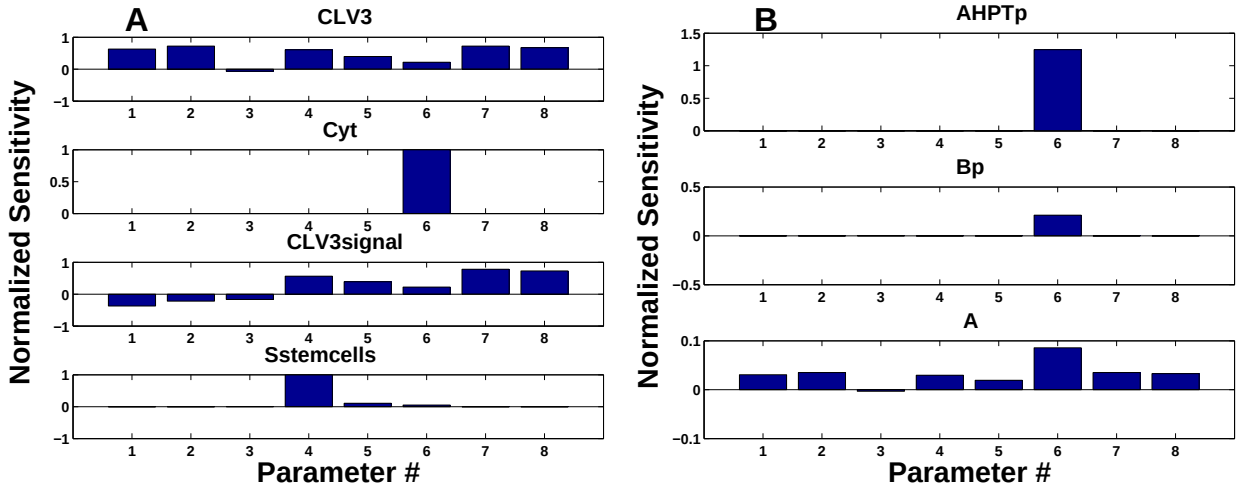

Figure 11: Sensitivity of CLV3, cytokinin, Sstemcells & CLV3signal to changes in all parameters in cell 11(Panel A). Sensitivity of AHPT-P, B-P & Type ARR signals to changes in all parameters in cell 11(Panel B)

a positive sensitivity, as seen in the bold line on species 4, which corresponds to CLV3 increase on increasing the production rate of CLV3.(2)Sstemcells production rate–CLV3, CLV3signal and Sstemcells display positive sensitivity. (3)cytokinin production rate–here not all cells display the same sensitivity, because not all cells have the same amount of signaling (stem cells have basal amounts of receptors).In particular, AHPT-p, B-p & WUS have positive sensitivity, whereas Type A ARR has negative sensitivity. One can see that the nature of the feedbacks makes several species sensitive to changes even in one parameter. In Figure M11A,B, which displays normalized sensitivity in cell 11, we see that in addition to WUS(Figure M9), cytokinin, AHPT-P, Type A ARR & B-P are all sensitive to changes in cytokinin production. Increasing cytokinin leads to more signal, hence higher B-p, AHPT-P, but lower Type ARR, since WUS represses Type ARR. Meanwhile increases in WUS lead to more Sstemcells. Also Sstemcells is sensitive to changes in its production which is expected.

Parameter distributions based upon random search

The above robustness study was local, namely we slightly perturbed parameter values, one at a time, and observed changes in species levels. Now we explore new parameter

sets, which could give similar/closely matched patterns. To collect other parameter sets, we first randomly generate a test parameter set, with each parameter value perturbed by $0.5 - 1.5$(uniformly distributed) its original fiducial value(Table M1). We use the Nelder-Mead (downhill simplex) [9] method for optimizing the parameters to fit the final expression patterns of WUS and CLV3, in the wild type(fiducial parameter set) for 30 cells. We chose to do this as, these species are crucial components of the network and also display high sensitivity to parameter changes. The error function is defined as,

$$error = (\sum_{i=1:30} [WUS(i) - WUS_0(i)]^2) + (\sum_{i=1:30} [CLV3(i) - CLV3_0(i)]^2) \tag{7}$$

With the starting initial random parameter set, we run the simplex until a certain tolerance is reached (i.e until the error does not decrease any further). We performed a Monte-Carlo simulation, by generating hundreds of parameter sets, the distributions of which are displayed in Figure M12A. The relative variance of the parameters are displayed in Figure M12B, by scaling the parameter values to unity. From here we see that the parameter that stands out as least robust is the cytokinin production rate. On the other hand, the other parameters are fairly robust.

CLV3 loss/gain of function

Throughout the text and supplementary figures, we assume that the "wild type" and CLV3 loss of function correspond to $b_2 = 1, 0.1$ respectively, unless mentioned otherwise (in Figure S5 A,B). To obtain the Figure S8 A,B, we assume same parameters as in Table M1, but with the change, $b_1 = 2$, which corresponds to higher transcriptional efficiency of the Type B ARR, in transcribing WUS. The CLV3 loss of function (Figure S8 B) is simulated for $b_2 = 0.01$. Figure S3 A, B, main text, for the CLV3 gain of function is obtained for $b_2 = 100$. As discussed in the main text, in Figure S3 B, CLV3 and WUS levels are small, which correspond to loss of meristem function. Here, cytokinin signaling is weak, even though

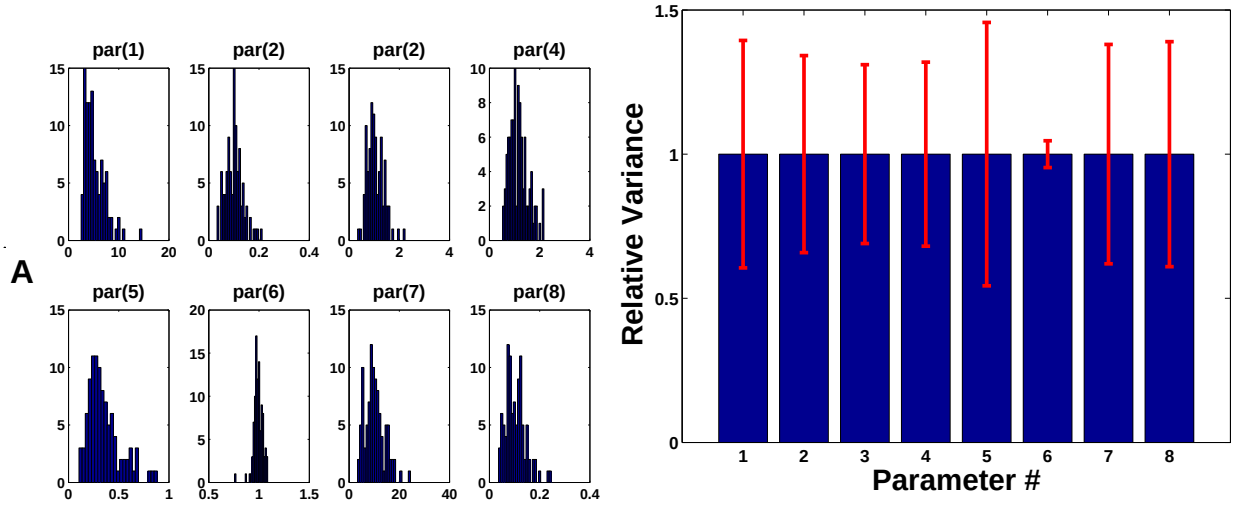

Figure 12: Histograms of parameter values for repeated simulations starting from random parameter guesses(left panel). Means and standard deviation of the parameter values(right panel)

cytokinin is present. The question is why this is so. The small amount of cytokinin signaling is enough to keep Type A ARRs at a high level(Figure M13). Type A ARRs negatively regulate cytokinin signaling and hence leads to low WUS levels. Since WUS is not able to suppress Type A ARR levels, this leads to the situation where cytokinin levels are high, but cytokinin signaling is low.

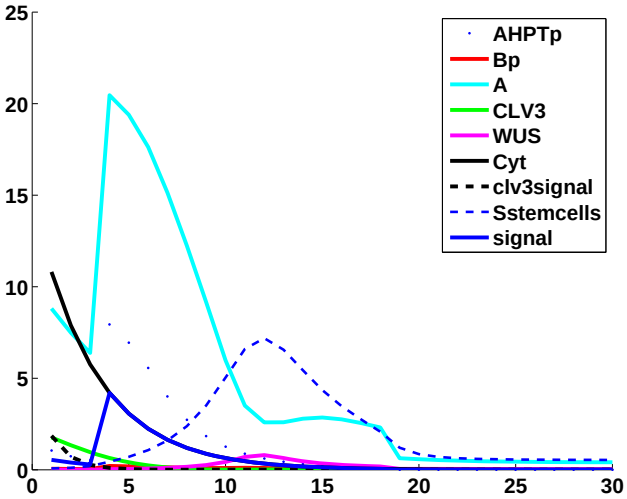

Figure 13: Network component expression as a function of cell numbers, for the CLV3gain of function mutant. Notice that Type A ARR is at a significantly high level, thereby ensuring that WUS is kept low.

TABLE1

K_{h1}	v_{h1}	K_{h2}	K_1	α	v_1	K_2	a_0	a_1	a_2	n	b_0
5	2	5	1	2	1	1	0.01	5	10	2	.001
b_1	b_2	α_1	d_s	α_2	d_1	d_2	α_3	d_w	C_r	a_c	r_c
0.25	1	10	0.1	5	0.1	1	1	0.33	1	0.5	1

Table 1: The concentration of the network components are in dimensionless units, the rate constants (transcription and degradation) are in units of min^{-1}, and the Michaelis-Menton constants are dimensionless. We assume no form of cooperativity unless specifically mentioned(we use $n = 2$, since multiple binding sites for WUS were found on the Type A ARR promoter [3]). Typical timescales of phosphorylation/de-phosphorylation time of the AHPTs are min, and time scales of induction of the Type A & Type B ARRs, are hrs [1]. Based on this we assume a degradation rate for the Type A ARR to be $0.025min^{-1}$. We also assume that all degradation rates $\gamma_i = 0.025min^{-1}$. Treatment of cytokinin is simulated by assuming an external fixed concentration of cytokinin($c_0 = 100$). To generate Figure 2 C, main text, we assume for the WUS mutant $b_1 = 0.125$.

References

[1] Gordon SP, Chickarmane VS, Ohno C, Meyerowitz EM. (2009)Multiple feedback loops through cytokinin signaling control stem cell number within the Arabidopsis shoot meristem.Proc Natl Acad Sci U S A. 106(38):16529-34.

[2] Muller, B. and Sheen, J., Advances in cytokinin signaling. Science 318 (5847), 68 (2007), see also Hwang, I. and J. Sheen, Two-component circuitry in Arabidopsis cytokinin signal transduction. Nature, 2001. 413(6854): p. 383-9; To JP, Kieber JJ.(2008) Cytokinin signaling: two-components and more. Trends Plant Sci. 13(2):85-92. To JP, Kieber JJ.

[3] Leibfried, A., et al., WUSCHEL controls meristem function by direct regulation of cytokinin-inducible response regulators. Nature, 2005. 438(7071): p. 1172-5.

[4] Moran U, Phillips R, Milo R. (2010)SnapShot: key numbers in biology. Cell 141(7):1262-1262.e1

[5] Shea MA, Ackers GK (1985) The OR control system of bacteriophage λ. A physical chemical model for gene regulation. *J Mol Biol* 181:211-230.

[6] Buchler NE, Gerland U, Hwa T (2003) On schemes of combinatorial transcription logic. *Proc Natl Acad Sci USA* 100:5136-5141.

[7] Bintu L, *et al.* (2005) Transcriptional regulation by the numbers: models. *Curr Opin Genet Dev* 15:116-124.

[8] Hasty J, Isaacs F, Dolnik M, McMillen D, Collins JJ (2001) Designer gene networks: Towards fundamental cellular control. Chaos 1: 207220.

[9] Nelder. J. A, Mead. R (1965) A Simplex Method for Function Maximization. Comput. J, 7:308-313.